

## Overexpression of CD133 Promotes Drug Resistance in C6 Glioma Cells

James M. Angelastro and Michael W. Lamé

### Abstract

Glioblastoma multiforme is an extremely aggressive and clinically unresponsive form of cancer. Transformed neoplastic neural stem cells, resistant to chemotherapy and radiation therapy, are thought to be responsible for the initial tumor formation and the recurrence of disease following surgical resection. These stem cells express multidrug resistance markers along with CD133. We show that ectopic overexpression of CD133 in rat C6 glioma cells leads to significant reluctance to undergo apoptosis from camptothecin and doxorubicin. Although p53 was upregulated in CD133-overexpressing glioma cells treated with DNA-damaging agents, apoptosis seems to be p53 independent. At least one ABC transporter, rat P-glycoprotein/ABCB1, was upregulated by 62% in CD133<sup>+</sup> cells with a corresponding increase in activity. Thus, the combination of higher P-glycoprotein mRNA transcription and elevated transporter activity seems to contribute to the protection from cytotoxic reagents. In conclusion, previous investigators have reported that resilient cancer stem cells coexpress CD133 and ABC transporters with increased reluctance toward apoptosis. Our data suggest that CD133 may contribute to the observed resistance to apoptosis of CD133<sup>+</sup> cancer stem cells. *Mol Cancer Res*; 8(8); 1105–15. ©2010 AACR.

### Introduction

Each year, brain tumors occur in 21,810 individuals, with astrocyte-derived glioma being the most prevalent. Among the four grades of gliomas, glioblastoma multiforme (GBM), WHO classification grade IV, is the most malignant and the least amenable to therapeutic intervention. GBMs regrow after surgical resection and contain a population of tumor cells resistant to radiation and chemotherapy. Recent advances in neural stem cell research found that brain tumors have a subpopulation of cancer stem cells, also called tumor-initiating cells, that contribute to radiation and chemotherapy resistance (1-23). Ignatova et al. (24) provided the first evidence for the existence of stem cells in human GBMs. These authors isolated clonogenic, neurosphere-forming precursor cells that expressed neuronal and astroglial markers upon differentiation. These cells also had altered expression of Delta, Jagged, and Survivin relative to normal neural stem cells located in the subventricular zone and dentate gyrus of the hippocampus. The neural stem cell-rich subventricular zone is suspected as the most probable origin of gliomas, with tumors arising following exposure to oncogenic viruses or

carcinogens (as reviewed by Sanai et al. in ref. 12). As defined by Vescovi et al. (5), to qualify as a brain tumor stem cell, the following criteria should be met: (a) orthotopic implantation results in a phenocopy of the original tumor; (b) brain tumor stem cells have extensive self-renewal properties; (c) cells have evidence of genetic or karyotypical alterations; (d) altered differentiation potential; (e) ability to generate nontumorigenic end cells; and (f) capacity to, but not necessarily retain the ability of multilineage differentiation. Cancer stem cells share many of the properties of their nonneoplastic counterparts (12). Both are self-renewable, drug resistant, and form spherical colonies in culture. (6, 10, 25-29). Drug resistance is often associated with elevated expression and activity of ABC transporters—identifiable markers for both normal neural and cancer stem cells (5, 30). An additional marker for both types of stem cells is the cell surface protein CD133 (8-10, 14, 31-33). Singh et al. (9) used the membrane topological location of CD133 to separate CD133<sup>+</sup> glioblastoma brain tumor stem cells from CD133<sup>-</sup> cells. On transplant, CD133<sup>+</sup> cells developed into xenographic tumors, but CD133<sup>-</sup> cells did not (9). CD133<sup>+</sup> stem cells have also been found in colorectal cancer, breast cancer, hepatocarcinomas, melanomas, and osteosarcomas (3, 6, 9, 13, 31, 34-37). Thus, CD133 could be one of the most successful biomarkers characterizing cancer stem cells.

CD133/prominin-1 was originally discovered in membrane protrusions on mouse neuroepithelial stem cells. CD133 is a five-transmembrane glycoprotein containing 865 amino acids. Its nonglycosylated molecular weight is 97 kDa, and its NH<sub>2</sub> terminus is extracellular with two extracellular loops, ending with a 56- to 59-amino-acid cytoplasmic tail (Swiss Prot O43490). There are five

**Authors' Affiliation:** Department of Molecular Biosciences, University of California, Davis, School of Veterinary Medicine, Davis, California

**Note:** J.M. Angelastro and M.W. Lamé contributed equally to this work.

**Corresponding Author:** James M. Angelastro, Department of Molecular Biosciences, University of California, One Shields Avenue, Davis, CA 95616. Phone: 530-752-1591; Fax: 530-752-4698. E-mail: jmangelastro@ucdavis.edu

doi: 10.1158/1541-7786.MCR-09-0383

©2010 American Association for Cancer Research.

potential glycosylation sites on the first extracellular loop and three sites on the second extracellular loop. Membrane topology has been suggested as the functional role for CD133 because it is found in cell membrane protrusions in intestinal microvillus and renal cells as well as protrusions, filopodia, and lamellipodia in the apical surface of neural epithelial cells (32, 38-42). CD133 has no known preferential ligands or connections with signaling pathways. In humans, CD133 dysfunction is associated with autosomal recessive retinal degeneration. A single nucleotide deletion and the resulting frameshift produce a truncated form lacking half the extracellular loop, the entire fifth transmembrane domain, and all the cytoplasmic tail. The resulting mutation leads to impaired photoreceptor disc morphogenesis and phenotypic retinal degeneration (32, 38, 39, 42, 43). In mice, a similar phenotype was observed with loss of CD133/prominin-1 (44).

The coincidental finding of CD133<sup>+</sup> cancer stem cells being resistant to chemotherapeutic-induced apoptosis led to our efforts to determine whether CD133 expression serves a functional role in triggering multidrug resistance (MDR) in glioma cells (45). To investigate this potential relationship, rat C6 glioma cells ectopically expressing CD133 were used. These cells normally do not have a major population positive for CD133 or ABC transporters (25, 27). We report that exogenous expression of CD133 promotes a 2- to 4-fold reduction in apoptosis resulting from therapeutic reagents camptothecin and doxorubicin. Exogenously expressed CD133 promoted more expression of Bax without apoptosis. Higher induction of p53 upon exposure to camptothecin was observed in CD133<sup>+</sup> cells, but the role of p53 in CD133<sup>+</sup> cells may serve to promote DNA repair rather than apoptosis. Finally, CD133<sup>+</sup> C6 cells have a 62% higher expression of at least one ABC transporter (known as ABCB1, P-glycoprotein), along with higher transporter activity, which leads to resistance to therapeutic reagents. Our findings support the hypothesis that CD133 plays an antiapoptotic functional role in protecting cancer cells; that is, cancer stem cells are protected from chemotherapy. These results support ongoing research to target CD133 as a means to eradicate cancer stem cells.

## Materials and Methods

### Materials

Cell growth medium DMEM with 4 mmol/L glutamine and 1 mmol/L pyruvate, fetal bovine serum (FBS), Lipofectamine 2000, TRIzol reagent, Superscript III, PureLink Quick Plasmid Miniprep kit, and pcDNA3.1/NT-GFP-TOPO vector kit were from Invitrogen. Expand High Fidelity<sup>Plus</sup> PCR system was from Roche. BCA protein assay reagent was from Thermo-Scientific. ECL Plus Western blotting detection system was from GE Healthcare. Camptothecin and doxorubicin anticancer drugs were from Sigma-Aldrich; each was dissolved in DMSO at 25 and 10 mmol/L, respectively.

### Cloning of rat CD133

The kidneys from a pentobarbital euthanized male Sprague-Dawley rat (200 g; Charles Rivers) was used as a source for CD133 as described by Weigmann et al. (46). The tissue was first freeze clamped and subsequently reduced to a fine frozen tissue dust with a liquid nitrogen-cooled mortar and pestle. Aliquots of 200 mg were then dissociated with TRIzol reagent (catalogue no. 15596-018, Invitrogen) according to the manufacturer's instructions. The upper layer containing the RNA was diluted with an equal volume of 70% ethanol, and total RNA was further purified using RNeasy Midi kit (catalogue no. 75142, Qiagen). The mRNA was obtained from the previous total RNA using an Oligotex mRNA midi Kit (catalogue no. 70042, Qiagen). To avoid degradation upon storage, the mRNA was immediately converted to cDNA using random hexamers and SuperScript III First-Strand Synthesis system (catalogue no. 18080-051, Invitrogen). CD133 was amplified from the cDNA by using Expand High Fidelity<sup>Plus</sup> PCR system (Roche) according to manufacturer's specifications using the following PAGE-purified forward primer 5'-ATGGCTCTCGTATT-CAGTGTCTGCT-3' (T<sub>m</sub> = 61.4°C) and reverse primer 5'-TCAGTATCGAGACGGGCTTGTCATAACAG-3' (T<sub>m</sub> = 61.0°C; Integrated DNA Technologies, Coralville IA). The amplification product was separated on a 1.0% SeaKem GTG Agarose gel (Lonza) in TAE buffer, and the band was extracted from the gel using a QIAquick Gel Extraction Kit (catalogue no. 28704; Qiagen). The product was inserted in-frame with green fluorescent protein (GFP) using the vector pcDNA3.1/NT-GFP-TOPO (catalogue no. 45-0247). The plasmid was introduced into TOP10 *Escherichia coli* and plated on Luria-Bertani broth medium agar containing 100 µg carbenicillin/mL. Colonies were screened for the correct plasmid insert size and orientation by PCR. Positive clones were expanded by growth in LB medium (100 µg/mL carbenicillin), and the plasmid was extracted for sequencing (Davis Sequencing) using PureLink Quick Plasmid Miniprep kit (catalogue no. K2100-10, Invitrogen). The sequence was identical to the National Center for Biotechnology Information database NM\_021751.2 for *Rattus norvegicus* prominin 1, except for wobble at position 2036 where G was substituted for A without alteration in amino acid identity.

Plasmid pcDNA3.1/NT-GFP without the CD133 insert, but still expressing GFP, was used as the transfected control (Invitrogen TOPO kit). To check for a fusion translated product, 293FT cells grown to near confluence in a 60-mm dish were transfected with pcDNA3.1/NT-GFP/CD133 fusion and Lipofectamine 2000 reagent (catalogue no. 11668-019, Invitrogen). This was done with a ratio of 8 µg plasmid to 20 µL of reagent according to the manufacturer's suggestion. After 48 hours, cells were gently washed with ice-cold PBS and lysed in 50 mmol/L Tris buffer (pH 7.4), 150 mmol/L NaCl, 1% NP40, 0.25% sodium deoxycholic acid, 0.1% SDS, 1× Protease Inhibitor Cocktail Set I (catalogue no. 539131, Calbiochem), 1 mmol/L NaF, and 1 mmol/L activated sodium

orthovanadate (radioimmunoprecipitation assay buffer). The reaction was allowed to progress on ice for 1 hour, and insoluble material was removed by centrifugation at  $16,000 \times g$  for 30 minutes. Protein was determined using the BCA protein assay reagent. Protein was separated on an 11% T:2.75% C SDS-PAGE gel and subsequently blotted using the tank method and Towbin buffer onto polyvinylidene difluoride membrane ( $0.2 \mu\text{m}$ , Bio-Rad). Membranes were subsequently blocked with 5% milk in 50 mmol/L Tris (pH 7.4) and 150 mmol/L NaCl for 1 hour at room temperature and then exposed to GFP rabbit antiserum (1/2,000, Invitrogen) overnight at  $4^\circ\text{C}$  in blocking buffer. Blots were washed three times for 5 minutes each with TBS and then exposed to donkey anti-rabbit conjugated to horseradish peroxidase (HRP;

1/5,000, catalogue no. NA934V, GE Healthcare) for 1 hour (room temperature) in blocking buffer. Blots were subsequently washed with 0.05% Tween 20 in TBS (5 minutes) and washed four times with TBS. Positive material was detected using the ECL Plus Western blotting detection system (catalogue no. RPN2132, Amersham-GE Healthcare). A positive fusion product was detected (Fig. 1) corresponding to a mass indicating a GFP fusion product and glycosylated CD133.

#### Transfection of C6-glioma cells

C6-glioma cells were dissociated by 0.05% trypsin 1 mmol/L EDTA and plated onto 24-well plates in DMEM with 4 mmol/L glutamine, 1 mmol/L pyruvate, 4.5 g/L, and 10% FBS medium. The next day, cells were transfected

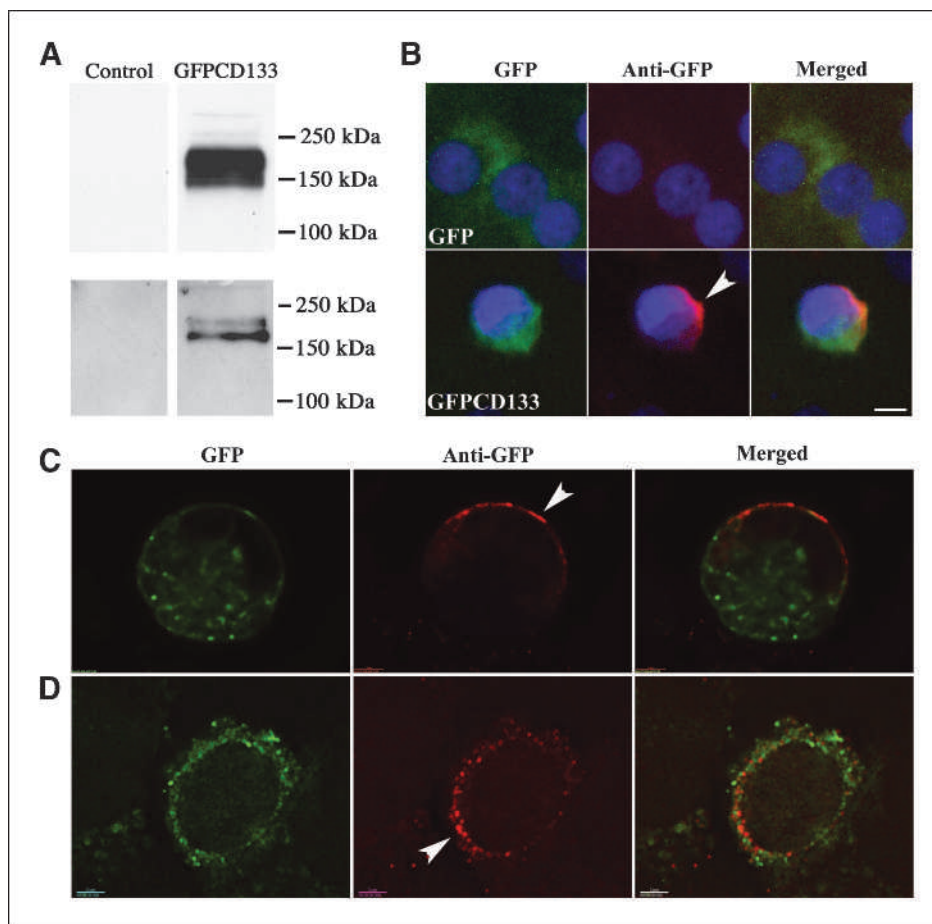


**FIGURE 1.** Western immunoblot of the 170 to 150 kDa GFP-CD133 fusion protein in C6 glioma cells. A, top, cell lysates, 50  $\mu\text{g}$  of protein, from 293FT cells that were control untransfected (left lane) and transiently transfected with pcDNA3.1/NT-GFP-CD133 fusion (right lane). Bottom, anti-GFP immunoprecipitates from 6.508 mg C6-GFP cell lysate (left lane) and 7.859 mg C6-GFP-CD133 cell lysate (right lane) were separated on SDS-PAGE and then transferred to a polyvinylidene difluoride membrane and stained with anti-GFP antibody. GFP-CD133 migrates between 150 and 250 kDa. Epifluorescence microscopy of GFP and GFP-CD133 expression in stably transfected C6-GFP (B) and C6-GFP-CD133 (B, bottom, C, and D) glioma cells, respectively. C6-GFP cells and C6-CD133 cells (not permeabilized) were immunostained with anti-GFP antibody (red), but also show an intrinsic GFP fluorescence (green). The chromatin was stained with 4',6'-diamidino-2-phenylindole. B, C6-GFP-CD133 cells exhibit robust polarized membrane staining with anti-GFP (red), but C6-GFP cells show minor detection with anti-GFP staining. C, deconvoluted optical section (0.1  $\mu\text{m}$ ) with anti-GFP staining (red) further confirms that GFP-CD133 occupies the cell membrane in a polarized manner with an intrinsic GFP fluorescent (green) overlay, or (D) uniform anti-GFP staining with more GFP-CD133 on one side of the cell. Interestingly, GFP-CD133 shows punctate membrane anti-GFP staining, whereas most of the intrinsic GFP signal is in the cytoplasm. Arrowhead shows polarized staining. Scale, 5  $\mu\text{m}$  (B) and 2  $\mu\text{m}$  (C, D).

with 2  $\mu$ g of pcDNA3.1/NT-GFP or pcDNA3.1/NT-GFP/CD133 plasmid per well and LipoFectamine 2000 as recommended by the supplier (Invitrogen). Dominant negative (d/n)-p53, 1  $\mu$ g pCIN-d/n-p53 (from Wei Gu, Columbia University, New York, NY), 0.5  $\mu$ g pQCxI-dsRed, and 5  $\mu$ L LipoFectamine 2000 were added per well to transfect C6-GFP and C6-GFP/CD133 cells in a 24-well plate. The C6 glioma cells were treated with the anticancer drugs 24 hours later.

#### Establishment of stably transfected C6-GFP control cells and C6-GFP/CD133 fusion protein cells

Permanent rat C6 glioma cell lines overexpressing rat CD133GFP fusion protein and GFP were created by transfecting 100-mm plates of confluent C6 glioma cells with 20  $\mu$ g of pcDNA3.1/NT-GFP/CD133 or pcDNA3.1/NT-GFP plasmid and LipoFectamine 2000 as recommended by Invitrogen. After 2 days, cells stably expressing GFP/CD133 or GFP were selected using 4 mg of G418 (Sigma) per milliliter of DMEM with 4 mmol/L glutamine, 1 mmol/L pyruvate, 4.5 g/L glucose, and 10% FBS. After several weeks, the surviving green fluorescent C6 cells expressing different levels of CD133GFP or GFP were expanded into 60-mm wells. Stably transfected C6 glioma cells were further expanded and passaged onto 100-mm tissue culture plates by 0.05% trypsin and 0.2 g/L of EDTA•4Na in Hanks' Balanced Salt Solution (as described above) with 2 mg/mL G418 to maintain expression levels of GFP/CD133 fusion or GFP. For cytotoxic drug experiments, stably transfected C6 glioma cells were plated onto 24-well plates without G418 and treated with drugs 24 hours later. To confirm translation of GFP/CD133 in stably transfected C6 cells, GFP control and GFP/CD133 cells were grown to confluency in 75-cm<sup>2</sup> flasks. The cells in each flask were scraped into PBS, sedimented, washed in PBS, and subsequently lysed in 2 mL of 1% Triton X-100 in 150 mmol/L NaCl and 50 mmol/L Tris buffer (pH 7.4) with 1 $\times$  Calbiochem Protease Inhibitor Cocktail Set I, 1 mmol/L NaF, and 1 mmol/L Na<sub>3</sub>VO<sub>4</sub> on ice for 1 hour. The lysates were centrifuged at 16,000  $\times$  g for 1 hour, and the supernatant protein was measured by BCA assays. For immunoprecipitation, 6.508 mg of protein from C6-GFP cells and 7.859 mg of protein from C6-GFP/CD133 cells were diluted to 12 mL with PBS in a conical centrifuge tube and allowed to rock for 4.5 hours at room temperature in the presence of Vector Fusion-Aid-GFP resin (50 mg). The resin was allowed to settle and was subsequently washed two times with PBS (12 mL).

Resin was resuspended in 2 $\times$  Laemmli sample buffer (100  $\mu$ L) and boiled for 2 minutes. The entire recovered supernatant for both GFP and GFP/CD133 were separated by SDS-PAGE and blotted as previously described. The blot was blocked with 5% milk for 1 hour, and then developed with 1  $\mu$ g/mL anti-GFP mouse monoclonal clone N86/8 (catalogue no. 75-131; nonprofit University of California Davis/National Institute of Neurological Disorders and Stroke/National Institute of Mental Health NeuroMab Facility) dissolved in 5% milk TBS overnight at

4°C. The blot was washed three times with TBS and then developed in 1/2,000 dilution of anti-mouse HRP from sheep in 5% milk for 1 hour, washed once with 0.05% Tween 20 TBS and three times with TBS, and developed with ECL plus reagent for 20 minutes. For cytotoxic drug experiments, the stably transfected C6 glioma cells were plated onto 24- or 96-well plates without G418 and treated with agents 24 hours later.

#### Western analysis of Bax, Bcl-2, and p53 from rat C6-glioma cells permanently transfected with GFP or GFP/CD133 in the presence and absence of camptothecin

Rat C6-glioma cells were cultured in DMEM (catalogue no. 11995, Gibco) with 10% FBS in 75-cm<sup>2</sup> flasks. Permanently transfected control cells containing GFP or GFP/CD133 were exposed to vehicle DMSO or 10  $\mu$ mol/L camptothecin for 6 days. Cells were scraped into the medium present in the flask at time of harvest to avoid the loss of potentially nonadherent or apoptotic cells. Then, cells were centrifuged in 15 mL conical tubes and washed with 12 mL of ice-cold PBS, sedimented by centrifugation, resuspended in PBS, transferred to 1.5 mL tubes, and lysed (radioimmunoprecipitation assay buffer). SDS-PAGE (50  $\mu$ g protein/lane), blotting, and exposures to primary and secondary antibodies were conducted as previously described. The following mouse monoclonal antibodies and concentrations were used: BCL2 (1/200, catalogue no. sc-7382, Santa Cruz Biotechnology), Bax (1/200, catalogue no. sc-7480, Santa Cruz Biotechnology), p53 (1/1,000, catalogue no. 1C12, Cell Signaling Technologies), and  $\beta$ -actin (1/5,000, catalogue no. A-5441, Sigma). The HRP-conjugated anti-mouse secondary antibody was from GE Healthcare (1/5,000, catalogue no. NXA931). The same blot was used for BCL2 and subsequently for Bax after stripping for 10 minutes (Restore Western Blot stripping buffer), rinsing with TBS, and reblocking.

#### Relative quantitation of MDR transporters in rat C6-glioma cells

Cells were grown (25-cm<sup>2</sup> flasks), treated, and harvested as described in the previous section. Isolation of RNA and conversion to cDNA was as described above, except that the material was not subjected to mRNA isolation. For real-time PCR, primers for rat ABCB1 (P-glycoprotein), ABCG2, Mrp2, and  $\beta$ -actin were designed using IDT free software (Table 1). Reactions were composed of 250 nmol/L of forward and reverse primers, 50 ng of total RNA (260:280 ratio above 1.9), and SYBR Green PCR Master Mix (catalogue no. 4309155, Applied Biosystems) in a total volume of 25  $\mu$ L. Samples, in triplicate, were developed using 7300 Real-time PCR System (Applied Biosystems) with default setting at 40 cycles and a dissociation stage with automatically set baselines and Ct threshold.

#### Fluorescence microscopy

C6-GFP/CD133 and C6-GFP glioma cells with and without 6-day camptothecin treatment were fixed in 4%

**Table 1.** List of quantitative real-time PCR templates with forward and reverse primers

Template	Forward primer	Reverse primer
ABCB1	5'-GCTTATGCGAAAGCTGGAGCAGTT-3'	5'-TGGCCGTGATGGCTTCTTTATGC-3'
ABCG2	5'-AAAGGATGTCTAAACAGGGCCGGA-3'	5'-GTGCTGGCCATGAAACATGAGTT-3'
Mrp2	5'-AACCGGAAGGTCAAGTTCTCCAT-3'	5'-TTGTCAGAGTCACTGGTCCAAGCA-3'
$\beta$ -Actin	5'-TGAGCGCAAGTACTCTGTGTGGAT-3'	5'-TAGAAGCATTTCGGTGCACGATG-3'

paraformaldehyde in PBS for 45 minutes at room temperature. After three washes with PBS, the cells were blocked in 10% goat serum with 1% Triton X-100 for anti-cleaved caspase-3/anti-GFP, or without Triton X-100 for single labeling with anti-GFP for 2 hours, and were immunolabeled overnight. The sections were subsequently incubated for 1 hour at 4°C with goat Alexa 488–conjugated anti-mouse/goat Alexa 568–conjugated anti-rabbit antibodies for anti-cleaved caspase-3/anti-GFP or goat Alexa 568–conjugated anti-mouse for single labeling with anti-GFP in 10% nonimmune goat serum.

Microscopy was done on either a Zeiss Axiovert 200 microscope (cleaved caspase-3/GFP) or a Delta Vision Deconvolution microscope (anti-GFP with intrinsic GFP single) at 0.1- $\mu$ m optical sections enhanced by Huygens Deconvolution Software. Images of xy and yz planes confirmed colocalization in cell sections.

#### Measurement of cell survival

Transfected or stably transfected C6-glioma cells were treated with 10  $\mu$ mol/L final concentration of camptothecin, 10 to 5  $\mu$ mol/L concentration of doxorubicin, or DMSO vehicle control with 1 mL of medium. Between 4 and 6 days, the growth medium was removed from each well and replaced with PBS containing 1  $\mu$ g/mL 4',6-diamidino-2-phenylindole and 0.1% Triton X-100, and exchanged with PBS after 10 minutes. GFP+ cells possessing condensed nuclei and fragmented chromatin were scored as apoptotic using Zeiss Axiovert 200 microscope. Data were presented as the proportion of GFP+ cells with apoptotic nuclei (47). Measurement of caspase-3/7 was performed using Apo-ONE Homogeneous Caspase-3/7 Assay kit according to the manufacturer's directions (Promega). Initial plating of cells was 50,000 per well of a 96-well plated with camptothecin at 10  $\mu$ mol/L or DMSO as the vehicle control. Assay was done 2.5 days after the initial treatment. Before the assay, cells were equilibrated for 30 minutes in EBM medium (Lonza, catalogue no. CC-3129) devoid of phenol red and containing EGM-2MV SingleQuots (Lonza, CC-4147). The assay was subsequently performed in this same medium.

#### Measurement of ABC transporter activity

Each of the stably transfected GFPCD133 and GFP C6 glioma cell lines were plated in 12 wells at  $1.7 \times 10^5$  cells per well. Calcein AM hydrolysis was measured from 0 to 24 minutes at 37°C in Molecular Devices SpectraMax M2 microplate counter. Calcein AM was added to the cells

according to the manufacturer's instructions (Invitrogen, Vybrant Multidrug Resistance Assay Kit, SKU V13180). Before the assay, cells were equilibrated for 30 minutes in EBM medium (Lonza, catalogue no. CC-3129) devoid of phenol red and containing EGM-2MV SingleQuots (Lonza, catalogue no. CC-4147). The assay was subsequently performed in this same medium.

#### Statistical analyses

Student's *t* test was used.

#### Results

##### Expression analysis of GFPCD133 shows SDS-PAGE apparent MW of 170 to 150 kDa

Transient transfection of 293FT cells and stably transfected C6 glioma cells with the GFPCD133 plasmid produced a fusion protein that migrated as a 170 to 150 kDa polypeptide (Fig. 1A). Cell lysates were used from 293FT cells, and immunoprecipitation was used from C6 glioma cells. A band was observed at the predicted molecular weight, corresponding to a fusion protein consisting of GFP (28,973 Da, GFP plus spacer amino acids) and glycosylated CD133. Nontransfected 293T cells and C6 glioma cells stably transfected with GFP were devoid of bands in this region (Fig. 1A). C6 glioma cells stably transfected with GFP (C6-GFP) or GFPCD133 (C6-GFPCD133) show green fluorescent cells from GFP in the cytosol; however, C6-GFPCD133 also showed green staining at the cell membrane (Fig. 1B). Previous investigators have reported the same locations, cytosol and cell membrane, for endogenous CD133 (48, 49). To confirm that GFPCD133 is membrane bound, C6-GFP and C6-GFPCD133 cells were fixed without membrane permeabilization and stained with anti-GFP antibody. C6-GFP cells revealed minor anti-GFP staining. By contrast, C6-GFPCD133 cells showed significant detection by the anti-GFP antibody at the cell membrane (Fig. 1B). Optical deconvoluted fluorescent microscopic sections substantiated our results by showing punctate red anti-GFP labeling at the membrane with overlay of the green GFP intrinsic signal (Fig. 1C and D). Granular formation of the GFP intrinsic signal within the cytoplasm most likely represents GFPCD133 expression in the endoplasmic reticulum as well as the Golgi, consistent with endoplasmic reticulum synthesis and Golgi processing and glycosylation of transmembrane proteins. In addition, membrane anti-GFP staining illustrated that GFPCD133 expression was polarized in cells (Fig. 1C)

and also showed detection throughout the cell membrane with preference on one side of the cell (Fig. 1D). CD133 protein has been shown to be distributed in the uropod of migrating hematopoietic stem and progenitor cells (50) and detected on the apical side of the glandular epithelia in membrane protrusions. Likewise, the apical of embryonic neural epithelia and epidermal cells of the adult brain that line the lateral ventricle also show apical staining of CD133 (46-53). When C6-GFP and C6-GFPCD133 cells were permeabilized by Triton X-100 and then stained with anti-GFP, both cell lines showed detection of cytosolic GFP (Fig. 2).

### Expression of GFPCD133 fusion protein promotes resistance to apoptosis resulting from anticancer drugs

Published findings showing CD133<sup>+</sup> cancer stem cells resistant to anticancer drugs led to our efforts to determine whether expression of CD133 promotes drug resistance. Cells grown in culture treated with the topoisomerase I inhibitor camptothecin promotes double-strand breaks in the cell DNA, which results in apoptosis. To examine whether exogenous expression of CD133 leads to protection of C6 glioma cells from camptothecin, C6 cells expressing GFP or stably transfected GFPCD133 were treated with camptothecin at 10  $\mu\text{mol/L}$ . Cells with condensed or fragmented chromatin were considered apoptotic and were shown to also stain positively for apoptotic marker cleaved caspase-3 (Fig. 2A) along with increased caspase-3/7 activity (Fig. 2B), which further corroborated that breakdown of chromatin serves as a reporter for drug-induced apoptosis. Stably transfected C6-GFP glioma cells showed apoptosis in 34% of the cells, whereas only 8% of the stably transfected C6-GFPCD133 cells were apoptotic within 6 days of treatment (Fig. 3A). The DMSO vehicle control showed 1% to 2% of the C6 cells expressing GFP or GFPCD133 undergoing apoptosis (Fig. 3A). Taken together, the exogenous

expression of CD133 evokes resistance to camptothecin-induced apoptosis in C6 glioma cells. Moreover, G418 selection did not lead to drug resistance in stably transfected C6 cells because stably transfected GFP cells were less resistant to camptothecin than stably transfected GFPCD133 cells.

The DNA synthesis inhibitor doxorubicin was next tested to determine whether exogenous expression of CD133 promotes drug resistance to more than one anticancer drug. For doxorubicin, 5 and 10  $\mu\text{mol/L}$  concentrations were used. The stably transfected GFP C6 cells revealed that 18% and 24% of cells were apoptotic for 5 and 10  $\mu\text{mol/L}$  doxorubicin, respectively. By contrast, stably transfected GFPCD133 C6 cells revealed that only 5.5% and 6.6% were apoptotic for 5 and 10  $\mu\text{mol/L}$  doxorubicin, respectively (Fig. 3B). The DMSO vehicle had only 2% to 3% apoptotic cells (Fig. 3B). Collectively, CD133 provided significant protection from apoptosis evoked by both camptothecin and doxorubicin.

### CD133 leads to higher tolerance for Bax before camptothecin treatment

To assess the mechanism of the CD133-induced protective action, the expression of proapoptotic Bax and antiapoptotic BCL2 were examined in C6-GFP and C6-GFPCD133 lines before and after camptothecin treatment. Oligomerization of Bax results in the formation of pores in the outer mitochondrial membrane, promoting the release of cytochrome *c*, whereas BCL2 binds to Bax and inhibits the formation of Bax oligomers. Thus, increasing the level of BCL2 to Bax (i.e., lower Bax/BCL2 ratio) promotes the mitochondrial retention of cytochrome *c*. Western immunoblot shows an apparent reduction of BCL2 after 6 days of camptothecin treatment both in C6-GFP and C6-GFPCD133 cells (Fig. 4A). In contrast, Bax protein levels are shown to be increased

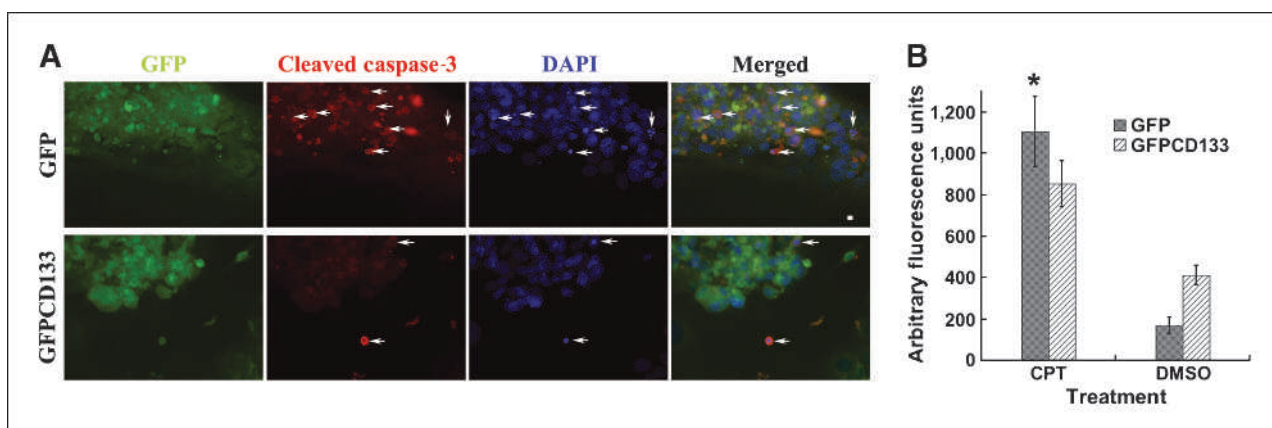


**FIGURE 2.** Positive cleaved caspase-3 immunostaining in cells with condensed or fragmented chromatin validates apoptosis. A, stably transfected C6-GFP and C6-GFPCD133 glioma cells grown on fibronectin-coated coverslips were treated with 10  $\mu\text{mol/L}$  camptothecin for 6 days and then were fixed and immunostained with anti-GFP and anti-cleaved caspase-3. Both C6-GFP and C6-GFPCD133 cells are GFP<sup>+</sup> (green), and arrows show apoptotic cells that are cleaved caspase-3<sup>+</sup> and have condensed and fragmented chromatin. Scale, 5  $\mu\text{m}$ . DAPI, 4',6'-diamidino-2-phenylindole. B, cleavage of z-DEVD-R110 to measure caspase-3/7 activity after 2.5 days of 10  $\mu\text{mol/L}$  camptothecin treatment of C6-GFP and C6-GFPCD133 cells. Results are given in arbitrary fluorescent units. \*, one-tailed Student's *t* test showed  $P = 0.045$  for camptothecin-treated C6-GFP versus camptothecin-treated C6-GFPCD133 cells.

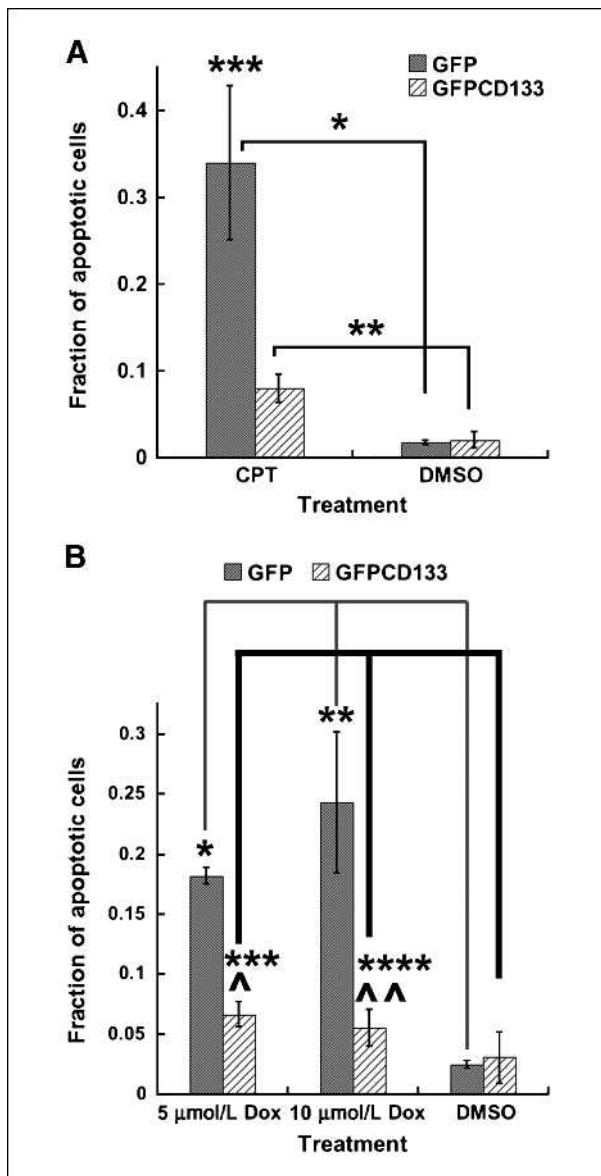


**FIGURE 3.** A, camptothecin (10 µmol/L) treatment of C6 glioma cells. Fraction of apoptotic cells from stably transfected C6-GFP or C6-GFPCD133 from treatment with 10 µmol/L camptothecin or DMSO. Values represent the mean ± SEM for three cultures in which at least 100 to 200 transfected cells were evaluated per culture. (Student's *t* test: \*, camptothecin-treated GFP versus DMSO-treated GFP cells,  $P = 0.011$ ; \*\*, camptothecin-treated GFPCD133 cells versus DMSO-treated GFPCD133,  $P = 0.019$ ; \*\*\*, camptothecin-treated GFP cells versus camptothecin-treated GFPCD133 cells,  $P = 0.025$ ). B, doxorubicin (Dox; 5 or 10 µmol/L) treatment of stably transfected C6-GFP and C6-GFPCD133 glioma cells. Fraction of apoptotic cells from stably transfected C6-GFP or C6-GFPCD133 from treatment with 10 µmol/L doxorubicin, 5 µmol/L doxorubicin, or DMSO. Doxorubicin treatment was for 5 days. Values represent the mean ± SEM for three cultures in which at least 100 to 200 transfected cells were evaluated per culture. Student's *t* test: doxorubicin-treated GFP versus DMSO-treated GFP cells at 5 µmol/L (\*,  $P = 1.57 \times 10^{-5}$ ) and at 10 µmol/L (\*\*,  $P = 0.011$ ); doxorubicin-treated GFPCD133 cells versus DMSO-treated GFPCD133 at 5 µmol/L (\*\*\*,  $P = 0.14$ ) and at 10 µmol/L (\*\*\*\*,  $P = 0.32$ ); doxorubicin-treated GFP cells versus doxorubicin-treated GFPCD133 cells at 5 µmol/L (^,  $P = 0.0003$ ) and at 10 µmol/L (^,  $P = 0.020$ ).

with camptothecin (Fig. 4A). The intensity of each protein band was digitally quantitated, and data are expressed as Bax/BCL2 ratios (Fig. 4B). The Bax/BCL2 protein ratio is shown to be statistically significant between untreated C6-GFP cells and untreated C6-GFPCD133 cells, with C6-GFPCD133 cells having a higher Bax/BCL2 ratio (Fig. 4B). By contrast, camptothecin-treated C6-GFPCD133 and C6-GFP cells have statistically insignificant ratios (Fig. 4B). The apparent higher Bax protein level along with less BCL2 expressed in the untreated C6-GFPCD133 cells seems to have led to the higher ratio shown in Fig. 4B, but without detectable increases in apoptosis compared with untreated C6-GFP cells (Fig. 3A). Taken together, the higher Bax expression along with caspase-3/7 activity (Fig. 2B) suggests that CD133 promotes reluctance for cells to undergo apoptosis.

### Camptothecin induces greater expression of p53 protein in C6-GFPCD133 cells than in C6-GFP cells

Camptothecin has been shown to upregulate p53 protein. Western immunoblotting shows that 6 days of camptothecin exposure led to higher levels of p53 protein in stably transfected C6-GFPCD133 cells compared with stably transfected C6-GFP glioma cells. In addition to the p53 protein, p21-22 bands were observed for camptothecin-treated and untreated cells, but were less intense for untreated cells (Fig. 4C). The p21-22 bands have been determined to be p53 cleavage products that have affinity for mitochondria and aid in initiating cytochrome *c* release (54). Digitally quantitated p53 Western blots revealed that C6-GFPCD133 cells have twice the expression of p53 compared with C6-GFP cells during camptothecin treatment (Fig. 4D). The higher level of p53 in the camptothecin-treated C6-GFPCD133 cells would suggest a greater induction for apoptosis. Our surprising reciprocal effect of high p53 levels with reduced apoptosis in C6-GFPCD133 cells compared with C6-GFP cells suggests that p53 may serve to stop the cell cycle for DNA repair rather than trigger apoptosis. Transfection of dominant-negative p53 into C6-GFP and C6-GFPCD133 cells revealed that the typical camptothecin-induced apoptosis was at least four times more prevalent in C6-GFP cells than in C6-GFPCD133 cells (Fig. 5). Thus, induction of apoptosis and CD133 protection are both independent of p53.

### C6-GFPCD133 cells have a higher initial level of ABCB1 (P-glycoprotein) mRNA transcripts and ABC transport activity than C6-GFP cells

Because MDR proteins have been shown to be expressed in CD133<sup>+</sup> cancer stem cells, this is thought to lead to protection from anticancer drugs. The levels of MDR mRNAs were next examined in C6-GFP and C6-GFPCD133 cells. Rat Mrp2, ABCB1 (Fig. 6A), and ABCG2 MDR mRNA transcript levels were quantitated by real-time PCR from both C6-GFP and C6-GFPCD133 cells. Mrp2 and ABCG2 were expressed significantly less than ABCB1 and did not show any significant difference between

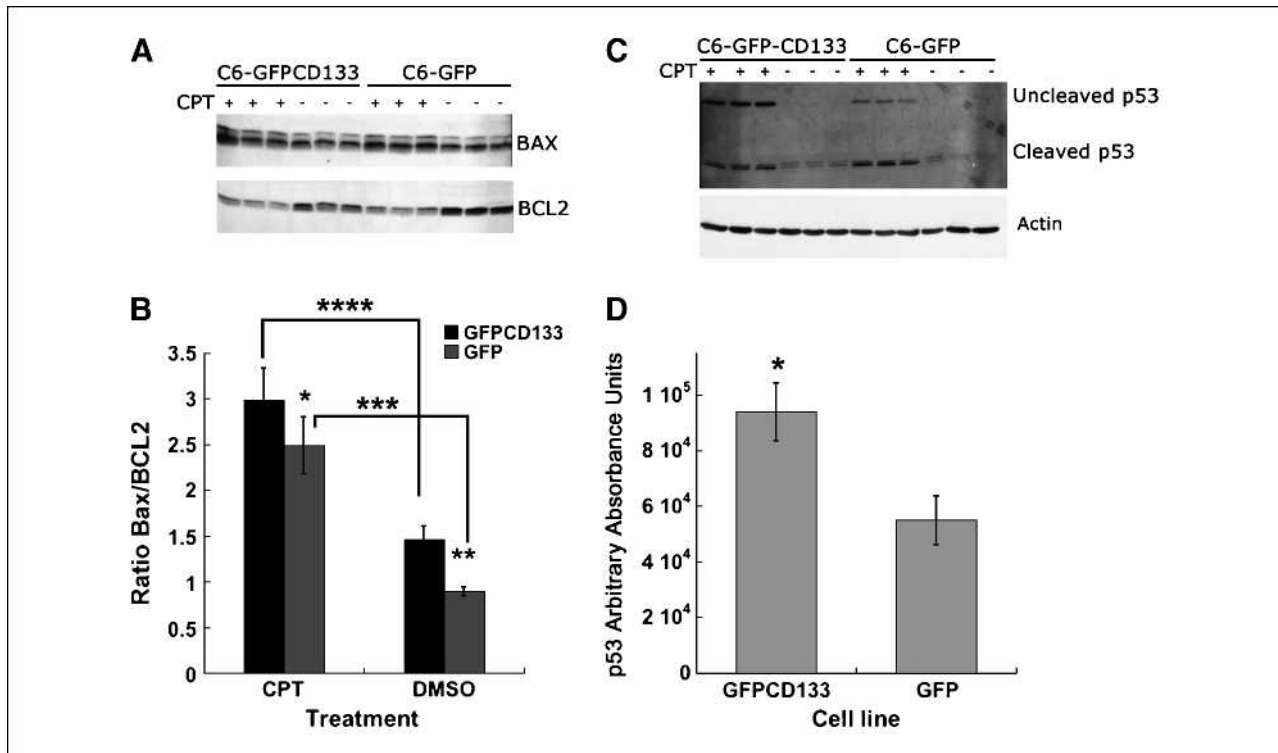


**FIGURE 4.** Bax, BCL2, and p53 ratio from camptothecin-treated stably transfected C6-GFP and C6-GFP/CD133 glioma cells at 10  $\mu\text{mol/L}$ . **A**, Western immunoblot probed with anti-Bax (top band) and then with anti-BCL2 (bottom band) for three individual C6-GFP/CD133 cultures treated with camptothecin (lanes 1–3) or with DMSO vehicle (lanes 4–6), and three individual C6-GFP cultures treated with camptothecin (lanes 7–9) or with DMSO vehicle (lanes 10–12). Cell lysate (50  $\mu\text{g}$ ) was added for each lane for SDS-PAGE and Western blot. **B**, Western blots were scanned and quantitated with densitometry. Bax/BCL2 values represent the mean  $\pm$  SD for three cultures (Student's *t* test: \*, camptothecin-treated Bax/BCL2 GFP versus camptothecin-treated Bax/BCL2 GFP/CD133,  $P = 0.14$ ; \*\*, Bax/BCL2 GFP versus Bax/BCL2 GFP/CD133,  $P = 0.004$ ; \*\*\*, camptothecin-treated Bax/BCL2 GFP versus Bax/BCL2 GFP/CD133,  $P = 0.0019$ ; \*\*\*\*, camptothecin-treated Bax/BCL2 CD133GFP versus Bax/BCL2 GFP/CD133,  $P = 0.0011$ ). **C**, camptothecin induces greater expression of p53 protein in C6-GFP/CD133 cells than in C6-GFP cells. Western immunoblot probed with anti-p53 (top blot) and then with anti- $\beta$ -actin (bottom blot) to show normalized sample loading for three individual C6-GFP/CD133 cultures treated with camptothecin (lanes 1–3) or with DMSO vehicle (lanes 4–6); and three individual C6-GFP cultures treated with camptothecin (lanes 7–9) or with DMSO vehicle (lanes 10–12). Cell lysate (50  $\mu\text{g}$ ) was added for each lane for SDS-PAGE. **D**, Western blot was scanned and quantitated by densitometry, and p53 values normalized against  $\beta$ -actin represent the mean  $\pm$  SD for three cultures (Student's *t* test: \*, camptothecin-treated GFP/CD133 p53 versus camptothecin-treated-GFP p53,  $P = 0.011$ ). Anti-p53 reveals full-length p53 and p21-22 p53-cleaved fragments.

C6-GFP and C6-GFP/CD133 cells. ABCB1 was present at a statistically significant 1.62-fold higher level in C6-GFP/CD133 cells compared with C6-GFP cells (untreated GFP versus untreated GFP/CD133;  $P = 0.0469$ ; Fig. 6B). Anticancer drugs are known to induce the expression of MDR mRNA transcripts and, as shown by 6-day camptothecin treatment, the expression of ABCB1 was induced 71-fold in C6-GFP and 41-fold in C6-GFP/CD133 cells (GFP/GFP/CD133, 71:41;  $P = 0.027$ ; Fig. 6B). A plausible explanation for the lower-fold change induction in C6-GFP/CD133 derives from the fact that C6-GFP/CD133 had a higher initial expression of ABCB1. In fact, the ratio of the ABCB1 fold-change between C6-GFP and C6-GFP/CD133 cell lines was 1.7, which is essentially the same as the initial fold difference between both cell lines before treatment (Fig. 6B). In addition, ABC transporter activity was measured by the influx of calcein AM into the C6 glioma cells. In the cytoplasm, esterases hydrolyze calcein AM from its hydrophobic chain, yielding a product

that fluoresces at 517 nm. The greater the ABC transporter activity, the less entry of calcein AM into the cytoplasm with less fluorescence. GFP/CD133 C6 glioma cells have less fluorescence compared with GFP C6 glioma cells (Fig. 6C). Thus, CD133 promotes upregulation of ABCB1 and higher ABC transporter activity.

## Discussion

*N*-nitrosomethylurea-derived rat glial tumor C6 cells have been used as a model for both astrocytoma tumors and cancer stem cells (25, 55). The majority of cultured C6 cells are considered to be cancer stem cells based on self-renewal properties, limited *in vitro* differentiation, and their ability to form tumors in nude mice (25). These cells also contain minor subpopulations that are CD133<sup>+</sup> and/or resistant to the cytotoxicity of Hoechst 33342. Cells that are resistant to Hoechst 33342 are often called side population cells, and ABCG2 transporter effluxes

Hoechst 33342 (45). By contrast, our work suggests that ABCB1 is the main efflux transport for camptothecin. However, the vast majority of C6 cells are sensitive to Hoechst 33342, lack MDR, and are not CD133<sup>+</sup> (27). Thus, the ectopic expression of CD133 in all C6 cells supports the role of this membrane protein as the key element for the development of xenobiotic resistance (25, 27). The higher expression of CD133 in transfected cells resulted in elevated MDR pump activity, supportive of a working relationship between these proteins. The possibility of CD133 accentuating the activity of MDR pumps is strengthened by their spatial relationship; MDR like CD133 is polarized to the apical membrane surface (56). We are presently in the process of determining the proximity of this relationship.

The results of the present study demonstrating that expression of CD133 elevates the resistance of C6 glioma cells to chemotherapeutic reagents strongly suggest the necessity for the implementation of therapeutic regimens that consider CD133 as a priority target. In fact, one investigation has used anti-CD133 monoclonal antibodies tagged with a therapeutic drug to destroy cancer stem cells. This approach may have had two consequences, one being the anticipated specific delivery of the therapeutic agent and second the unexpected enhancement of the efficacy of agents by interfering with CD133 through antibody-antigen binding (34).

A CD133 knockout mouse has been reported, which verified its role in photoreceptor disc formation (44). How-

ever, a functional role for CD133 on cytotoxic resistance has not yet been established in this knockout mouse. Biological roles for CD133 could be inferred from its physical properties. CD133 is found in cholesterol-rich lipid rafts within membrane protrusions of epithelium cells that could allow recruitment of ABC transporters to the raft for efflux transport of toxic compounds. Protrusions also allow greater surface area for more effluxing transporters to occupy. In contrast to this scenario, one investigation revealed that in leukemia cells, expression and activity of MDR (P-glycoprotein) was unaffected with or without protrusions and large folding of the cell membrane (57).

Lipid rafts have been shown to generate plasma membrane topology for signal transduction. Thus, CD133 may not carry out ligand binding itself, but it is involved in lipid raft formation for attracting ligand-binding receptors that integrate intracellular signal transduction pathways. Evidence for cell signaling is shown by 62% induction in the elevation of MDR-ABCB1 (P-glycoprotein) mRNA in C6-GFP/CD133 cells before addition of camptothecin. This induction could be explained by the discovery that exogenous CD133 triggered a signaling pathway for mRNA transcription. Alternately, the plasma membrane topology, formulated by CD133, could allow more redistribution of ABCB1 to the membrane and/or provide a better environment for efficient pump activity. Nonetheless, direct or indirect signaling has been shown to be carried out by CD133. In support of cell signaling, C6-GFP/CD133 cells were shown to have a higher Bax and lower BCL2 expression compared with C6-GFP cells without cytotoxic treatment. Exogenous CD133 expression in C6 cells seems to have contributed to the above, and the cells were shown to be more reluctant to undergo apoptosis with more Bax and less BCL2. Bax bound to BCL2 in the presence of camptothecin prevents initiation of apoptosis. Taken together, exogenously expressed CD133 increased ABCB1 mRNA with more Bax and reduced BCL2 protein. These data support the inference that CD133-directed regulation promotes increased MDR and greater reluctance to undergo apoptosis.

The increase of ABCB1 with higher ABC transporter activity in C6-GFP/CD133 does not necessarily mean that all the camptothecin is prevented appreciable access to the cell, as access is probably necessary to affect the increased production of p53. High levels of p53 have been shown to lead to apoptosis; however, it also promotes cell cycle arrest necessary for DNA repair, which could translate into the apoptotic resistance observed by C6-GFP/CD133 cells. However, use of dominant-negative p53 in CD133<sup>+</sup> cells did not result to cell death upon drug challenge; therefore, p53 production does not explain drug resistance. Finally, p53 protein has been shown to be deleted or mutated in 70% of glioblastomas (58). Consequently, these data provide evidence that CD133<sup>+</sup> cancer stem cells would be resistant to chemotherapy even with a disrupted p53 pathway.

In summary, our findings show that CD133 has a functional role in regulating cytotoxic resistance in C6 glioma

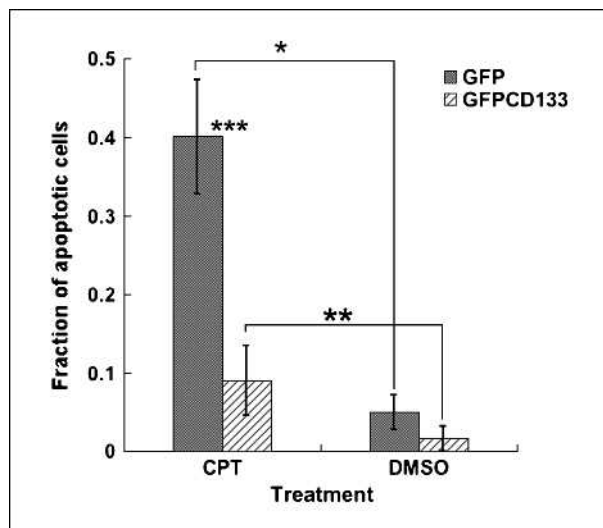


**FIGURE 5.** Camptothecin (10  $\mu\text{mol/L}$ ) treatment of C6-GFP and C6-GFP/CD133 glioma cells transfected with pCIN-d/n-p53 and pQCx-I-DsRED (2:1 ratio). Fraction of apoptotic cells from stably transfected C6-GFP or C6-GFP/CD133 from treatment with 10  $\mu\text{mol/L}$  camptothecin or DMSO. Camptothecin treatment was for 6 days. Values represent the mean  $\pm$  SEM for three cultures in which at least 100 to 200 transfected cells were evaluated per culture. (Student's *t* test: \*, camptothecin-treated GFP versus DMSO-treated GFP cells,  $P = 0.005$ ; \*\*, camptothecin-treated GFP/CD133 cells versus DMSO-treated GFP/CD133,  $P = 0.013$ ; \*\*\*, camptothecin-treated GFP cells versus camptothecin-treated GFP/CD133 cells,  $P = 0.011$ ).

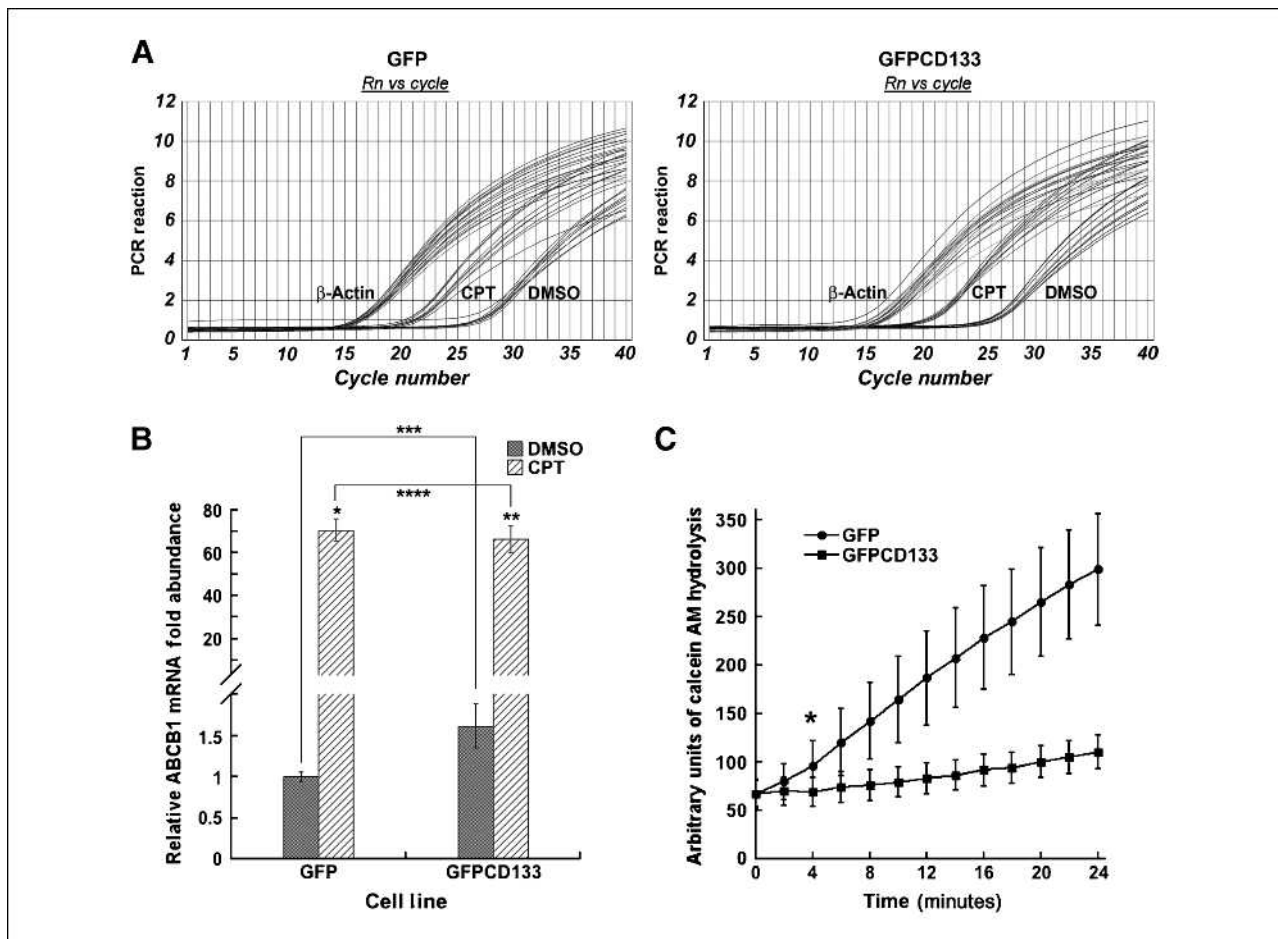


**FIGURE 6.** Relative P-glycoprotein mRNA before and after camptothecin treatment, and activity measurements of P-glycoprotein in C6 cells permanently transfected with GFP or GFPCD133. A, quantitative real-time PCR curves of C6-GFP (left) and C6-GFPCD133 (right) treated with DMSO vehicle or 10  $\mu$ M/L camptothecin. Treatment was achieved in three trials, and three PCR reactions were accomplished for each trial. Corresponding  $\beta$ -actin PCR curves were used to normalize input cDNAs by subtracting actin Ct values from P-glycoprotein Ct values. B, relative P-glycoprotein mRNA abundance based on DMSO-treated C6-GFP with the lowest level, which is compared with the abundance of mRNA with camptothecin-treated C6-GFP and C6-GFPCD133 cells as well as DMSO-treated C6-GFPCD133 cells (Student's *t* test: \*, camptothecin-treated GFP versus DMSO-treated GFP cells,  $P = 7.33 \times 10^{-5}$ ; \*\*, camptothecin-treated GFPCD133 cells versus DMSO-treated GFPCD133,  $P = 0.000237$ ; \*\*\*, DMSO-treated GFP cells versus DMSO-treated GFPCD133 cells,  $P = 0.0469$ ; \*\*\*\*, camptothecin-treated GFP cells versus camptothecin-treated GFPCD133 cells,  $P = 0.552$ ). C, hydrolysis of calcein AM from 0 to 24 minutes. Values represent the mean  $\pm$  SD for 12 wells. \*, Student's *t* test revealed statistical significance starting at 4 minutes with a  $P = 0.0046$ . Duplicate wells of C6-GFP and C6-GFPCD133 without calcein AM were measured to determine background emission from GFP. Background fluorescence from C6 cell lines did not change during the 24-minute assay. Therefore, GFP did not contribute to increasing calcein signal detection.

cells. Such regulation seems to be in part due to increasing the level of ABCB1 with ABC transporter activity, and by a p53-independent reluctance to enter into apoptosis. Therapeutic intervention to target CD133 combined with traditional chemotherapy reagents could formulate a treatment to ubiquitously eradicate cancer stem cells along with their tumor progeny.

## References

- Zhang QB, Ji XY, Huang Q, Dong J, Zhu YD, Lan Q. Differentiation profile of brain tumor stem cells: a comparative study with neural stem cells. *Cell Res* 2006;16:909–15.
- Zeppenick F, Ahmadi R, Campos B, et al. Stem cell marker CD133 affects clinical outcome in glioma patients. *Clin Cancer Res* 2008;14:123–9.
- Yi JM, Tsai HC, Glockner SC, et al. Abnormal DNA methylation of CD133 in colorectal and glioblastoma tumors. *Cancer Res* 2008;68:8094–103.
- Wang J, Sakariassen PO, Tsinkalovsky O, et al. CD133 negative glioma cells form tumors in nude rats and give rise to CD133 positive cells. *Int J Cancer* 2008;122:761–8.

## Grant Support

NIH, National Cancer Institute (J.M. Angelastro).

The costs of publication of this article were defrayed in part by the payment of page charges. This article must therefore be hereby marked *advertisement* in accordance with 18 U.S.C. Section 1734 solely to indicate this fact.

Received 08/24/2009; revised 05/27/2010; accepted 06/10/2010; published OnlineFirst 07/27/2010.

5. Vescovi AL, Galli R, Reynolds BA. Brain tumour stem cells. *Nat Rev Cancer* 2006;6:425–36.
6. Tirino V, Desiderio V, d'Aquino R, et al. Detection and characterization of CD133<sup>+</sup> cancer stem cells in human solid tumours. *PLoS ONE* 2008;3:e3469.
7. Thon N, Damianoff K, Hegemann J, et al. Presence of pluripotent CD133(+) cells correlates with malignancy of gliomas. *Mol Cell Neurosci* 2008;43:51–9.
8. Singh SK, Clarke ID, Terasaki M, et al. Identification of a cancer stem cell in human brain tumors. *Cancer Res* 2003;63:5821–8.
9. Singh SK, Hawkins C, Clarke ID, et al. Identification of human brain tumour initiating cells. *Nature* 2004;432:396–401.
10. Singh S, Dirks PB. Brain tumor stem cells: identification and concepts. *Neurosurg Clin N Am* 2007;18:31–8, viii.
11. Schrot RJ, Ma JH, Greco CM, Arias AD, Angelastro JM. Organotypic distribution of stem cell markers in formalin-fixed brain harboring glioblastoma multiforme. *J Neurooncol* 2007;85:149–57.
12. Sanai N, Alvarez-Buylla A, Berger MS. Neural stem cells and the origin of gliomas. *N Engl J Med* 2005;353:811–22.
13. Salnikow AV, Kusumawidjaja G, Rausch V, et al. Cancer stem cell marker expression in hepatocellular carcinoma and liver metastases is not sufficient as single prognostic parameter. *Cancer Lett* 2008;275:185–93.
14. Perez Castillo A, Aguilar-Morante D, Morales-Garcia JA, Dorado J. Cancer stem cells and brain tumors. *Clin Transl Oncol* 2008;10:262–7.
15. Liu W, Shen G, Shi Z, et al. Brain tumour stem cells and neural stem cells: still explored by the same approach? *J Int Med Res* 2008;36:890–5.
16. Kondo T. Stem cell-like cancer cells in cancer cell lines. *Cancer Biomark* 2007;3:245–50.
17. Kang MK, Hur BI, Ko MH, Kim CH, Cha SH, Kang SK. Potential identity of multi-potential cancer stem-like subpopulation after radiation of cultured brain glioma. *BMC Neurosci* 2008;9:15.
18. Joo KM, Kim SY, Jin X, et al. Clinical and biological implications of CD133-positive and CD133-negative cells in glioblastomas. *Lab Invest* 2008;88:808–15.
19. Hassan HT, Zhai X, Goodacre JA. CD133 stem cells in adult human brain. *J Neurooncol* 2008;89:247–8; author reply 249.
20. Gunther HS, Schmidt NO, Phillips HS, et al. Glioblastoma-derived stem cell-enriched cultures form distinct subgroups according to molecular and phenotypic criteria. *Oncogene* 2008;27:2897–909.
21. Dell'Albani P. Stem cell markers in gliomas. *Neurochem Res* 2008;33:2407–15.
22. Beier D, Wischhusen J, Dietmaier W, et al. CD133 expression and cancer stem cells predict prognosis in high-grade oligodendroglial tumors. *Brain Pathol* 2008;18:370–7.
23. Altaner C. Glioblastoma and stem cells. *Neoplasma* 2008;55:369–74.
24. Ignatova TN, Kukekov VG, Laywell ED, Suslov ON, Vrionis FD, Steindler DA. Human cortical glial tumors contain neural stem-like cells expressing astroglial and neuronal markers *in vitro*. *Glia* 2002;39:193–206.
25. Zheng X, Shen G, Yang X, Liu W. Most C6 cells are cancer stem cells: evidence from clonal and population analyses. *Cancer Res* 2007;67:3691–7.
26. Shervington A, Lu C. Expression of multidrug resistance genes in normal and cancer stem cells. *Cancer Invest* 2008;26:535–42.
27. Shen G, Shen F, Shi Z, et al. Identification of cancer stem-like cells in the C6 glioma cell line and the limitation of current identification methods. *In Vitro Cell Dev Biol Anim* 2008;44:280–9.
28. Hambardzumyan D, Squatrito M, Holland EC. Radiation resistance and stem-like cells in brain tumors. *Cancer Cell* 2006;10:454–6.
29. Bao S, Wu Q, McLendon RE, et al. Glioma stem cells promote radioresistance by preferential activation of the DNA damage response. *Nature* 2006;444:756–60.
30. Borst P, Jonkers J, Rottenberg S. What makes tumors multidrug resistant? *Cell Cycle* 2007;6:2782–7.
31. Singh SK, Clarke ID, Hide T, Dirks PB. Cancer stem cells in nervous system tumors. *Oncogene* 2004;23:7267–73.
32. Mizrak D, Brittan M, Alison MR. CD133: molecule of the moment. *J Pathol* 2008;214:3–9.
33. Fargeas CA, Huttner WB, Corbeil D. Nomenclature of prominin-1 (CD133) splice variants—an update. *Tissue Antigens* 2007;69:602–6.
34. Smith LM, Nesterova A, Ryan MC, et al. CD133/prominin-1 is a potential therapeutic target for antibody-drug conjugates in hepatocellular and gastric cancers. *Br J Cancer* 2008;99:100–9.
35. Woodward WA, Sulman EP. Cancer stem cells: markers or biomarkers? *Cancer Metastasis Rev* 2008;27:459–70.
36. Wright MH, Calcagno AM, Salcido CD, Carlson MD, Ambudkar SV, Varticovski L. Brca1 breast tumors contain distinct CD44<sup>+</sup>/CD24<sup>-</sup> and CD133<sup>+</sup> cells with cancer stem cell characteristics. *Breast Cancer Res* 2008;10:R10.
37. LaBarge MA, Bissell MJ. Is CD133 a marker of metastatic colon cancer stem cells? *J Clin Invest* 2008;118:2021–4.
38. Jaszai J, Fargeas CA, Florek M, Huttner WB, Corbeil D. Focus on molecules: prominin-1 (CD133). *Exp Eye Res* 2007;85:585–6.
39. Corbeil D, Roper K, Weigmann A, Huttner WB. AC133 hematopoietic stem cell antigen: human homologue of mouse kidney prominin or distinct member of a novel protein family? *Blood* 1998;91:2625–6.
40. Corbeil D, Roper K, Fargeas CA, Joester A, Huttner WB. Prominin: a story of cholesterol, plasma membrane protrusions and human pathology. *Traffic* 2001;2:82–91.
41. Roper K, Corbeil D, Huttner WB. Retention of prominin in microvilli reveals distinct cholesterol-based lipid micro-domains in the apical plasma membrane. *Nat Cell Biol* 2000;2:582–92.
42. Shmelkov SV, St Clair R, Lyden D, Rafii S. AC133/CD133/Prominin-1. *Int J Biochem Cell Biol* 2005;37:715–9.
43. Maw MA, Corbeil D, Koch J, et al. A frameshift mutation in prominin (mouse)-like 1 causes human retinal degeneration. *Hum Mol Genet* 2000;9:27–34.
44. Zaccagna S, Oh H, Wilsch-Brauninger M, et al. Loss of the cholesterol-binding protein prominin-1/CD133 causes disk dysmorphogenesis and photoreceptor degeneration. *J Neurosci* 2009;29:2297–308.
45. Dean M, Fojo T, Bates S. Tumour stem cells and drug resistance. *Nat Rev Cancer* 2005;5:275–84.
46. Weigmann A, Corbeil D, Hellwig A, Huttner WB. Prominin, a novel microvilli-specific polytopic membrane protein of the apical surface of epithelial cells, is targeted to plasmalemmal protrusions of non-epithelial cells. *Proc Natl Acad Sci U S A* 1997;94:12425–30.
47. Angelastro JM, Canoll PD, Kuo J, et al. Selective destruction of glioblastoma cells by interference with the activity or expression of ATF5. *Oncogene* 2006;25:907–16.
48. Immervoll H, Hoem D, Sakariassen PO, Steffensen OJ, Molven A. Expression of the “stem cell marker” CD133 in pancreas and pancreatic ductal adenocarcinomas. *BMC Cancer* 2008;8:48.
49. Saigusa S, Tanaka K, Toyama Y, et al. Correlation of CD133, OCT4, and SOX2 in rectal cancer and their association with distant recurrence after chemoradiotherapy. *Ann Surg Oncol* 2009;16:3488–98.
50. Giebel B, Corbeil D, Beckmann J, et al. Segregation of lipid raft markers including CD133 in polarized human hematopoietic stem and progenitor cells. *Blood* 2004;104:2332–8.
51. Pfenninger CV, Roschupkina T, Hertwig F, et al. CD133 is not present on neurogenic astrocytes in the adult subventricular zone, but on embryonic neural stem cells, ependymal cells, and glioblastoma cells. *Cancer Res* 2007;67:5727–36.
52. Karbanova J, Missol-Kolka E, Fonseca AV, et al. The stem cell marker CD133 (prominin-1) is expressed in various human glandular epithelia. *J Histochem Cytochem* 2008;56:977–93.
53. Coskun V, Wu H, Bianchi B, et al. CD133<sup>+</sup> neural stem cells in the ependyma of mammalian postnatal forebrain. *Proc Natl Acad Sci U S A* 2008;105:1026–31.
54. Sayan BS, Sayan AE, Knight RA, Melino G, Cohen GM. p53 is cleaved by caspases generating fragments localizing to mitochondria. *J Biol Chem* 2006;281:13566–73.
55. Benda P, Lightbody J, Sato G, Levine L, Sweet W. Differentiated rat glial cell strain in tissue culture. *Science* 1968;161:370–1.
56. Scoazec JY, Bringuier AF, Medina JF, et al. The plasma membrane polarity of human biliary epithelial cells: *in situ* immunohistochemical analysis and functional implications. *J Hepatol* 1997;26:543–53.
57. Radel S, Fredericks W, Mayhew E, Baker R. P-glycoprotein expression and modulation of cell-membrane morphology in Adriamycin-resistant P388 leukemia cells. *Cancer Chemother Pharmacol* 1990;25:241–6.
58. Collins VP. Brain tumours: classification and genes. *J Neurol Neurosurg Psychiatry* 2004;75 Suppl 2:ii2–11.

# Molecular Cancer Research

## Overexpression of CD133 Promotes Drug Resistance in C6 Glioma Cells

James M. Angelastro and Michael W. Lamé

*Mol Cancer Res* 2010;8:1105-1115. Published OnlineFirst July 27, 2010.

**Updated version** Access the most recent version of this article at:  
doi:[10.1158/1541-7786.MCR-09-0383](https://doi.org/10.1158/1541-7786.MCR-09-0383)

**Cited articles** This article cites 58 articles, 13 of which you can access for free at:  
<http://mcr.aacrjournals.org/content/8/8/1105.full#ref-list-1>

**Citing articles** This article has been cited by 2 HighWire-hosted articles. Access the articles at:  
<http://mcr.aacrjournals.org/content/8/8/1105.full#related-urls>

**E-mail alerts** [Sign up to receive free email-alerts](#) related to this article or journal.

**Reprints and Subscriptions** To order reprints of this article or to subscribe to the journal, contact the AACR Publications Department at [pubs@aacr.org](mailto:pubs@aacr.org).

**Permissions** To request permission to re-use all or part of this article, use this link  
<http://mcr.aacrjournals.org/content/8/8/1105>.  
Click on "Request Permissions" which will take you to the Copyright Clearance Center's (CCC) Rightslink site.